

Investigation of the β -Limit in the W7-AS Stellarator

A. Weller 1), J. Geiger 1), M. Zarnstorff 2), E. Sallander 1), S. Klose 1), A. Werner 1), J. Baldzuhn 1), R. Brakel 1), R. Burhenn 1), H. Ehmler 1), F. Gadelmeier 1), L. Giannone 1), D. Hartmann 1), R. Jaenicke 1), J. Knauer 1), H.P. Laqua 1), C. Nührenberg 1), E. Pasch 1), N. Rust 1), E. Speth 1), D.A. Spong 3), F. Wagner 1), U. Wenzel 1), W7-AS Team 1), NBI-Group 1)

- 1) Max-Planck-Institut für Plasmaphysik, IPP-Euratom Association,
D-85748 Garching, D-17489 Greifswald, D-10117 Berlin, Germany
2) Princeton Plasma Physics Laboratory, Princeton, NJ 08543, USA
3) Oak Ridge National Laboratory, Oak Ridge, TN 37831-8071, USA

e-mail contact of main author: arthur.weller@ipp.mpg.de

Abstract. A significant increase of the volume averaged beta from $\langle\beta\rangle \approx 2\%$ up to $\langle\beta\rangle > 3\%$ was achieved in W7-AS after modifications of the neutral beam injection (NBI) system and the installation of divertor structures. In particular, the favourable properties of high-iota configurations could be exploited by using the divertor control coils for eliminating edge islands. MHD-quiescent, quasi-stationary discharges at low radiation levels and with favourable confinement properties can be maintained. Experimental studies of equilibrium effects and of MHD mode activity have been performed with the X-ray tomography system for a variety of magnetic configurations. In addition results of computational MHD stability studies are presented, which show an increase of stability with increasing beta due to the pressure induced deepening of the magnetic well along with increasing magnetic shear, in qualitative agreement with experimental data. Under typical conditions the maximum achieved beta is still limited by the available heating power and not by equilibrium or stability effects. If the plasma is pushed close to the density limit or in the case of significant toroidal current drive MHD instabilities may cause a deterioration of the confinement. The reduced beta obtained in low-iota configurations is attributed to the equilibrium β limit due to a critical Shafranov shift associated with enhanced transport.

1. Introduction.

Major research goals for the advanced stellarator Wendelstein 7-AS include understanding the limit for the plasma beta and verifying the optimization of the magnetic configuration (reduced Pfirsch-Schlüter currents). In previous experiments [1] volume averaged β -values of up to $\langle\beta\rangle \approx 2\%$ could be achieved in the W7-AS stellarator with ≈ 3.5 MW balanced neutral beam power injected through the ports. The heating efficiency of the counter-injected beams was very poor as a consequence of low magnetic fields (0.7...1.25 T) and high density required to reach the maximum β -values. Under these particular conditions very large orbit losses occur resulting in heating efficiencies of $\eta \equiv P_{\text{abs}}/P_{\text{inj}} \approx 15\text{...}60\%$ only for counter-injected ions in the particular range of magnetic fields.

The previous high- β studies were preferentially conducted with an external rotational transform (vacuum iota with no current or pressure) in the range of $\iota_{\text{ext}}(a) \approx 0.34\text{...}0.45$ in order to avoid a reduction of the plasma radius by edge islands leading to reduced confinement, lower temperatures and higher radiation losses. The maximum achievable plasma β was not limited by MHD instabilities but rather by increasing radiation losses from the plasma core resulting from an uncontrollable density increase and impurity accumulation effects preventing the achievement of quasi-stationary discharges.

In order to enhance the plasma performance in the high- β regime and to investigate the stability limits, a rearrangement of the injectors [2] was made in such a way as to inject the NBI power in the co-direction only. The new segmented divertor consisting of 10 divertor modules (on top and bottom centered in the elliptical plane of each field period) [3,4] provides better control of the interaction with the plasma facing components but causes a reduction of the effective plasma radius from typically $a_{\text{eff}} \approx 17\text{...}18$ cm to $a_{\text{eff}} \approx 15$ cm in the low-iota regime ($\iota(a) \leq 0.5$), where smooth flux surfaces exist up to the limiting structures. Another consequence of the divertor is a limited flexibility to control the plasma position in

order to compensate for the Shafranov shift or to vary the magnetic well depth. The aim of the present experiments is to achieve higher β -values and to study the β -limit under these new experimental boundary conditions.

2. Optimization and Characterization of High- β Plasma Performance.

The present studies focused on the range around $\tau_{\text{ext}} = 0.5$ because of better equilibrium and confinement properties (Shafranov shift $\propto \tau^2$, equilibrium β -limit $\propto \tau^2$, $\tau_{E,ISS95} \propto \tau^{0.4}$). The control coils have been used to compensate the edge islands so that the effective plasma radius is comparable with the low-iota case. Therefore, actual island divertor configurations were not used in most of the experiments. Nevertheless a beneficial effect of the divertor was found resulting in improved density control and relatively low radiation losses. This is mainly attributed to the effective screening of the plasma by the large area graphite plasma facing components.

Scans of plasma parameters (density) and of configuration parameters (external rotational transform τ_{ext} , current of control coils I_{cc} , vertical field B_z , mirror ratio I_5/I_m , ohmic current I_{OH}) have been performed at the reduced magnetic field of $B = 1.25$ T in order to find optimum conditions. Besides the usual case of gas puffing used to vary the density pellet and fast gas injection has been applied. However, the flat top value of the plasma energy obtained with gas puffing could not be exceeded. A significant

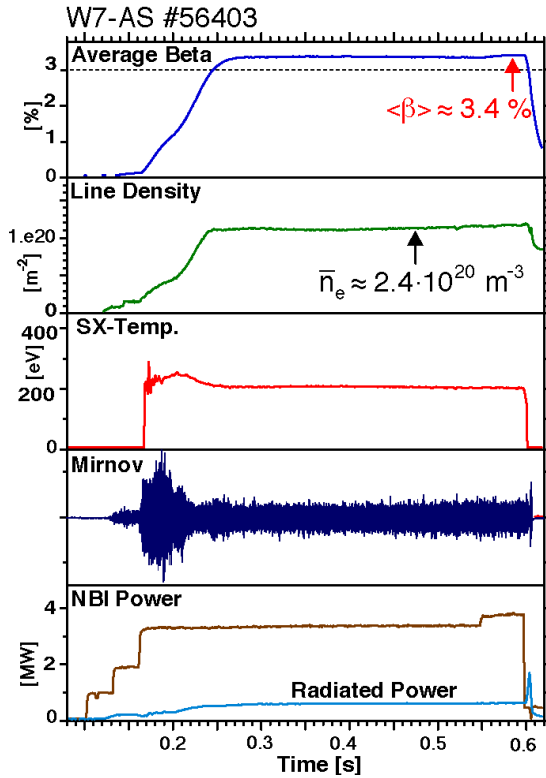


FIG. 2. Optimized quasi-stationary high- β discharge at 0.9 T, $\tau_{\text{ext}} = 0.52$, with $\langle\beta\rangle$ reaching 3.4 %. The (low) radiation losses are peaked at the plasma edge.

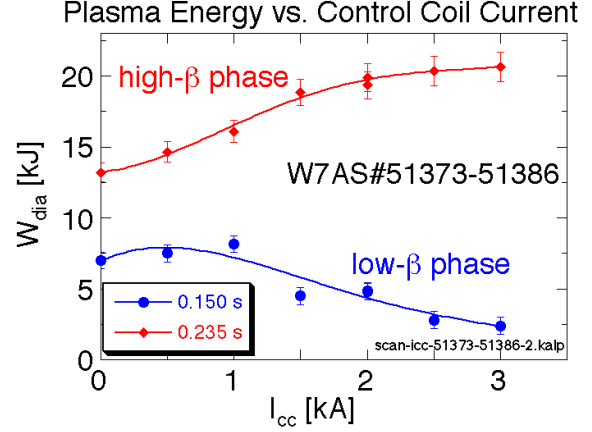


FIG. 1. Scan of control coil current. The polarity is chosen for compensation of edge islands. Opposite effects on the plasma energy are observed in the low- and high- β phases ($B = 1.25$ T, $\tau = 0.52$).

increase of the plasma energy could be achieved by using the divertor control coils as shown in *FIG. 1* resulting in a larger plasma volume. The optimum I_{cc} , however, is much larger than the calculated value required for compensating the resonant $(m,n) = (10,5)$ edge islands in the vacuum configuration. Therefore, the reduction of the plasma energy at low β (*FIG. 1*) is likely caused by overcompensated islands. Conversely, the beneficial effect in the high- β phase is an indication for the compensation of pressure induced islands at lower rational τ -values since the edge rotational transform is lowered (see next section). Such a conjecture is supported by the measured patterns of the H_{α} -light emission and of the heat deposition on the divertor plates (from infrared camera measurements), which show a transition from narrow structures in the case of $I_{\text{cc}} = 0$ (typical for configurations bounded by edge islands intersecting the divertor plates) to broad structures (typical for smooth surfaces almost aligned with the target plates in the poloidal cross section). The increase of the plasma volume is also reflected in a widening of electron density and temperature profiles measured in the edge region.

Central temperatures are in the range of $T_{e0} = 300...450$ eV. The density profiles are relatively broad and flat, typical line averaged densities are around $\langle n_e \rangle \approx 2...3 \cdot 10^{20} \text{ m}^{-3}$. The density has to be kept in an optimum range. At lower densities the energy confinement deteriorates, and at the same time, impurity accumulation effects take place. Towards higher densities, good confinement properties, similar to the High Density H-Mode (HDH) are achieved. This regime was first found in proper island divertor configurations [3,4]. In particular, the particle confinement times deduced from iron laser blow-off measurements in the $B = 1.25$ T case are in the range of ≤ 20 ms, corresponding to values of $\tau_p/\tau_e \leq 2.5$ only. However, beyond a critical density, the energy confinement saturates or even deteriorates due to approaching the density limit [5] caused by decreasing temperatures along with increasing radiation. The kinetic plasma energy deduced from plasma temperature and density profiles (with the assumption of $T_i = T_e$) is found to be in quantitative agreement with the measured diamagnetic plasma energy.

The maximum β was obtained with further decreased magnetic fields. The B-scan between 0.7...1.25 T typically gives a shallow optimum between 0.8...1.0 T. FIG. 2 shows an optimized case at $B = 0.9$ T, where values up to $\langle \beta \rangle \approx 3.4$ % (with central values of $\beta(0) \approx 7$ %) could be achieved for a flat top time of ≈ 0.35 s. The global energy confinement times are 25...50 % above the ISS-95 scaling [6] and close to the W7-95 scaling [6].

As far as the dependence of the achievable plasma β in net-current free discharges on the external rotational transform is concerned, the optimum is found in the vicinity of $\iota_{\text{ext}}(a) = 0.5$ (FIG. 3). In all cases, the achieved beta is not limited by macroscopic instabilities, but by confinement. In the range from $\iota_{\text{ext}}(a) = 0.46$ down to $\iota_{\text{ext}}(a) = 0.35$ the confinement deteriorates. This may be explained mainly by the decrease of the equilibrium β -limit (next section) towards low iota associated with enhanced transport. On the other hand, if the rotational transform is raised above $\iota_{\text{ext}}(a) = 0.53$, the global confinement degrades likewise to some extent, since the structure of the edge islands becomes more complicated, and therefore, the control coils cannot completely restore the maximum plasma radius.

3. Equilibrium Effects.

Despite of the reduction of $\langle j_{\parallel} / j_{\perp} \rangle$ relatively large vertical fields in the range of $B_z/B \geq 0.02$ have to be used in order to keep the high- β configuration well centered in the divertor troughs.

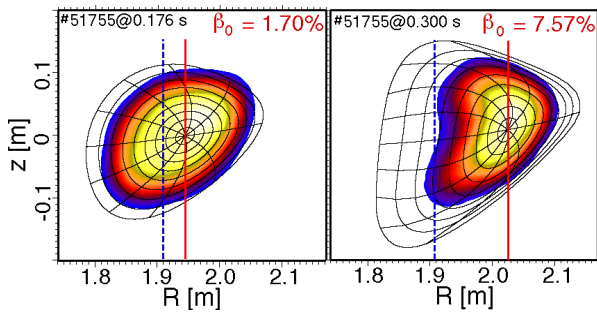


FIG. 4. Comparison of X-ray tomograms for #51755 ($\iota_{\text{ext}} = 0.52$) at low and high β compared with flux surfaces calculated by NEMEC (dashed line: axis position of the vacuum configuration).

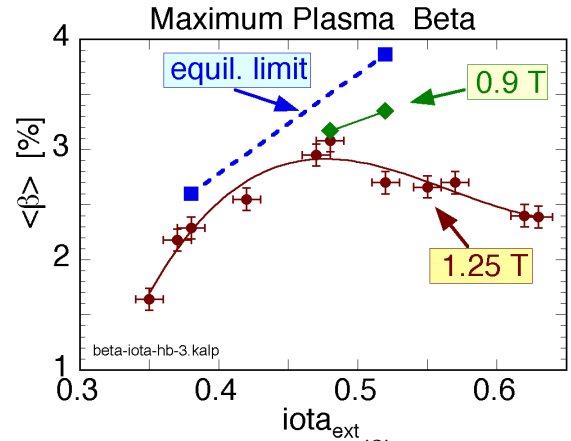


FIG. 3. The deterioration of $\langle \beta \rangle$ at low iota may be due to equilibrium limit effects. At high iota, residual edge islands may be present.

The volume averaged β was determined by equilibrium calculations with the VMEC and NEMEC codes [7]. The β -values are up to ≈ 7 % lower, if the diamagnetic effect is not taken into account. The change of the equilibria due to the Shafranov shift is illustrated in FIG. 4, where tomographic reconstructions of X-ray measurements are compared with calculations. At high β -values typically some indentation of the X-ray contours is found, which depends on β and central iota. This may be due to a significant axis shift, particularly in cases of a decreased

rotational transform in the center, caused by the ohmic current, which compensates the bootstrap and Okhawa currents. These internal current distributions were not taken into account in the NEMEC calculations. The axis positions deduced from the X-ray tomograms reflect the expected values and dependence on $\beta \cdot \tau^2$ despite of some offset in the experimental data (FIG. 5). The maximum normalized Shafranov shift at $\tau_{\text{ext}} \approx 0.52$ reaches $\Delta/r_h \approx 0.43$ (r_h is the horizontal radius of the flux surfaces) in the plane of highest elongation ($\phi = 36^\circ$). Therefore, the experimentally achieved β -values are still below the assumed equilibrium β -limit of $\approx 3.8\%$ corresponding to $\Delta/r_h = 0.5$. The critical β for the configuration with $\tau_{\text{ext}} \approx 0.38$ is noticeably reduced ($\approx 2.6\%$), and also in this case the experimentally achieved values stay slightly beneath this (FIG. 3). The pressure induced changes of the magnetic configurations are accompanied by the formation of significant shear and magnetic well, and therefore, implications on the MHD stability properties are expected.

4. MHD Stability - Experimental Studies in net-current free plasmas -

Under optimum conditions the plasmas with highest β -values show only weak MHD-activity, mostly coherent modes in the range 4...20 kHz. These low frequency modes are usually attributed to pressure driven modes around low order rational surfaces. During the transition to high- β , in particular at lower densities, global Alfvén gap modes (AEs) with frequencies up to ≈ 300 kHz can be excited [1]. They disappear, however, with increasing density, where the fast ion content is reduced.

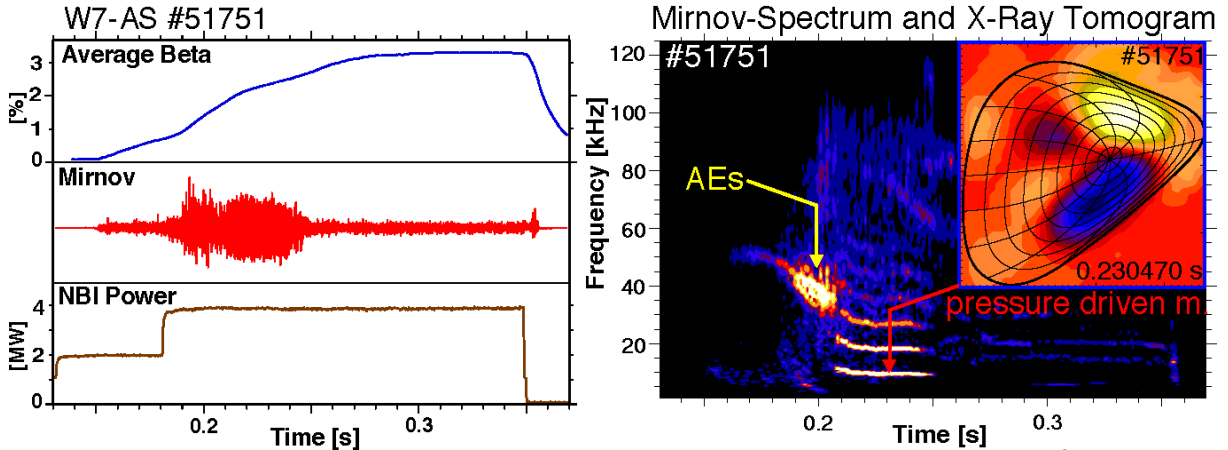


FIG. 6. : Low frequency $(m,n) = (2,1)$ mode activity during the transition into the high- β regime. The mode structure (inset: X-ray tomogram, fluctuating part of emissivity) shows a significant ballooning behaviour. After 0.25 s (where $\langle\beta\rangle > 2.5\%$) the discharge is very quiescent ($B = 0.8$ T, $\tau_{\text{ext}} = 0.52$).

The MHD-activity due to pressure driven modes is more pronounced at intermediate β -values. FIG. 6 illustrates the MHD behaviour of a discharge with parameters similar to the case shown in FIG. 2, in which the plasma β rises until $t \approx 0.3$ s. The 10 kHz mode activity measured by a magnetic probe (with harmonics at 20 and 30 kHz) ceases at 0.25 s, where $\langle\beta\rangle \approx 2.5\%$ is exceeded. The mode is identified as an $(m,n) = (2,1)$ mode by X-ray tomography. The radial position of the perturbation is consistent with the position of $\tau = 1/2$, which is progressively shifted inward with increasing β -induced shear. The experimental data suggest, that the stability improves with increasing β up to the maximum achieved values.

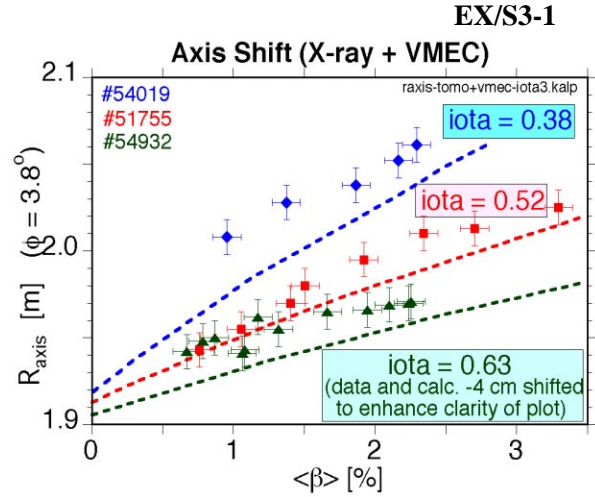


FIG. 5. Plasma axis position from X-ray analysis (symbols) depending on beta and iota in comparison with calculations (dashed lines).

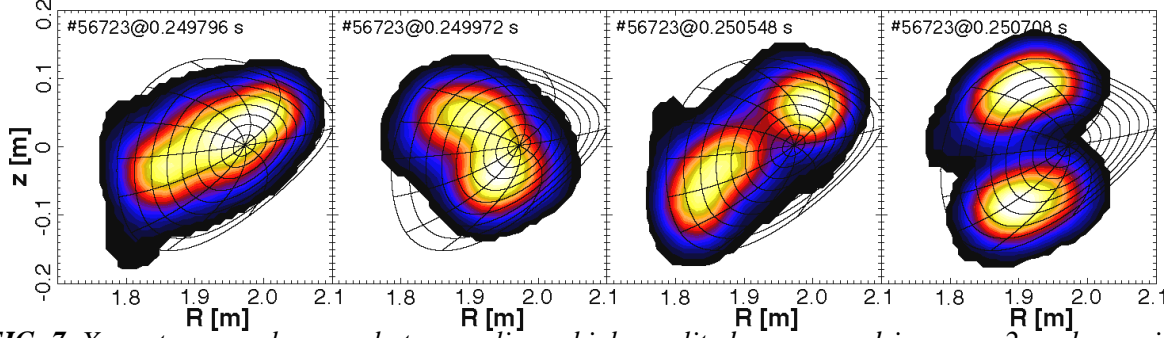


FIG. 7. X-ray tomography snapshots revealing a high amplitude pressure driven $m = 2$ mode causing a transient splitting of the hot plasma core before a partial collapse takes place in the low β phase ($\tau_{\text{ext}} = 0.48$).

Only in a few cases a transient deterioration of the confinement by these low frequency modes has been observed during the low- β phase. FIG. 7 shows an $m = 2$ mode, which causes the plasma to split into a doublet configuration and to lock just before a partial collapse, which indicates a resistive nature. However, the plasma did not terminate, but proceeded to $\beta \approx 3\%$ with additional heating power. Other discharges show MHD bursts causing very fast ($\approx 100 \mu\text{s}$) crashes of the plasma energy. Low temperatures with $T_e(0) \approx 200 \text{ eV}$, and therefore higher resistivity, typically obtained close to the radiative density limit, seem to play a key role in combination with particular configuration parameters, eg. large vertical fields or enhanced modular field ripple, leading to reduced stability. Not all of the observed phenomena are yet well understood. However, in general they have no impact on the confinement, and the discharges are typically very quiescent in the high- β phase.

5. MHD Stability - Computational Studies -

The configuration with $\tau_{\text{ext}} = 0.52$ corresponding to the case of best high- β performance has been chosen as a reference case for computational stability studies. In a first step a sequence of equilibria differing in $\langle\beta\rangle$ was calculated by the NEMEC code, using model pressure profiles. At low beta the iota profile is approximately flat with iota close to $1/2$. At $\langle\beta\rangle \approx 3\%$ the profile has tokamak-like shear with $\iota(0) \approx 0.54$ and $\iota(a) \approx 0.40$.

The local stability has been studied by evaluating the Mercier- and resistive interchange criteria with the JMC code [8] for each case. The stability diagrams (FIG. 8) exhibit an unstable region throughout the plasma cross section at very low β as a consequence of the relative large inward shift. The stable regions expand progressively towards the edge with increasing plasma β due to the increase of magnetic well depth and shear. Beyond the experimentally accessible β the stable regions shrink again. An unstable region at the edge persists throughout the range of β ($\langle\beta\rangle \approx 0 \dots 4.4\%$), which is particularly large for resistive interchange modes. The shift of $\iota = 1/2$ towards the plasma center along with a shift into the stable region occurs below the maximum β -value reached in this configuration corresponding

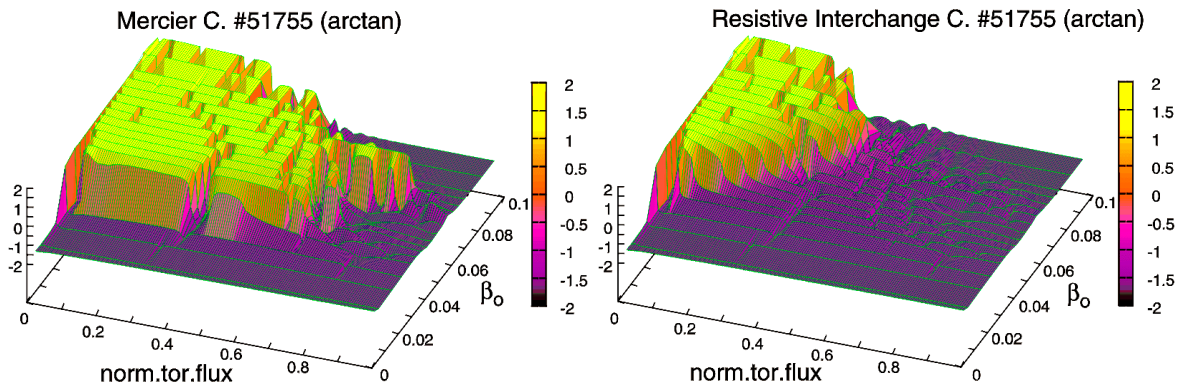


FIG. 8. Mercier- and resistive interchange stability diagram as a function of the central β value (equilibrium sequence for the case of $\tau_{\text{ext}} = 0.52$, #51755). Positive values of the stability parameter (z -axis) indicate stable regions. Unstable resonances are seen embedded in the stable region.

to $\langle\beta\rangle \approx 3\%$. This is consistent with the experimental data showing an $m=2$ mode activity at intermediate β -values, which disappears for $\langle\beta\rangle > 2\%$ (FIG. 6). For this case the most stable equilibrium corresponds to $\langle\beta\rangle \approx 3\%$. Above this value the unstable region at the plasma edge starts to grow again to some extent.

The global mode stability has been studied with the CAS3D ideal MHD stability code [9]. The free boundary calculations were done for the $N=1$ mode family perturbation including external modes with up to 64 perturbation harmonics taking the fluid compression into account. FIG. 9 shows the physical growth rates of unstable modes as a function of $\langle\beta\rangle$ in the lower part. Perturbed pressure contours are given in the inset for a particular case showing the global character of the eigenfunction and the dominating $(m,n) = (2,1)$ mode structure. All the perturbations are manifestly external as indicated by the peaking of the eigenfunctions at the plasma boundary. The results indicate that the existence of unstable, external, global modes is correlated to $\tau = 1/2$ in the plasma. The calculated growth rates decay with increasing β , again in qualitative agreement with the experimental observations. The reason for the peak in the growth rates at $\langle\beta\rangle = 2.1\%$ is the occurrence of the natural resonance $\tau = 5/11$ at the plasma boundary (see top of FIG. 9).

The local stability against high- n ideal ballooning modes has been investigated with the COBRA code [10] for 3 equilibria out of a similar sequence used in the calculations discussed above. In the calculations 15 field lines on each flux surface with different starting points have been examined. The ballooning calculations were truncated after 60 periods of good and bad curvature in order to focus on moderately localized modes. FIG 10 shows the effect of the equilibrium β on the calculated growth rates for a field line providing the highest average growth rate (but which is still negative apart from the edge region). Again, stability increases as β is raised, indicating a second stability type of behaviour. This could be due to an increase of the local poloidal field at the outboard side induced by the Shafranov shift causing a shorter connection length for field lines through the bad curvature region. Computational studies on resistive modes could possibly lead to a better understanding of the observed MHD phenomena. However, results are not yet available.

6. High- β Discharges with significant net Toroidal Currents

The main objectives of the experiments with significant net currents in W7-AS were to study the effect of additional rotational transform and shear on confinement and equilibrium in the high- β regime and to investigate the influence of rational surfaces and shear on pressure

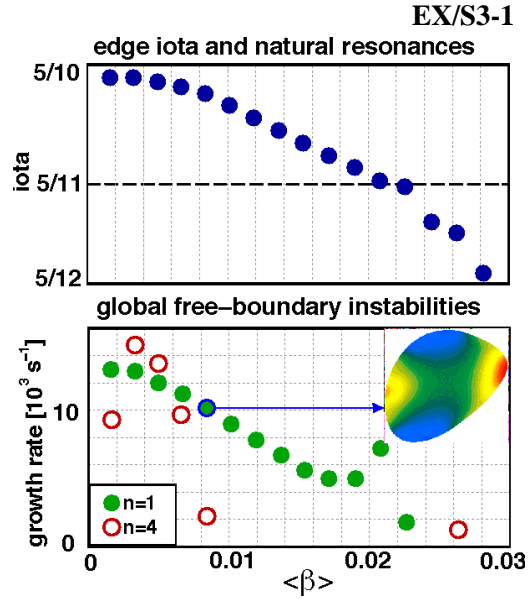


FIG. 9. Dependence of growth rates of unstable modes on β (from CAS3D for W7-AS case #51755), perturbed pressure contours (inset) and edge rotational transform (top).

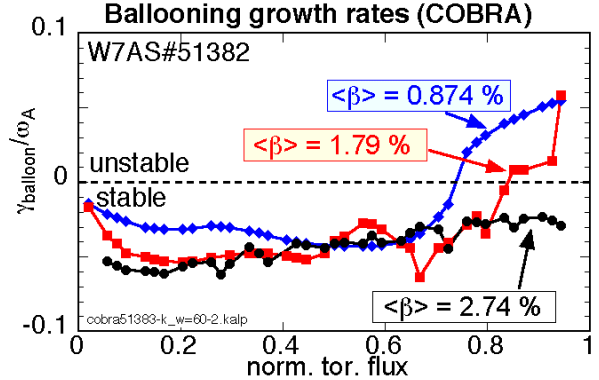


FIG. 10. : Local ideal ballooning mode stability for equilibria with $\langle\beta\rangle = 0.87, 1.8$ and 2.7% ($\tau_{ev} = 0.52$). The stability increases with β . (COBRA with $k_w = 60$ for most unstable fieldline).

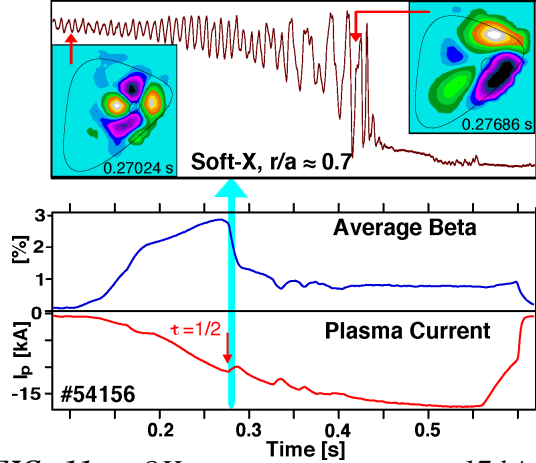


FIG. 11. : OH-current ramp up to -17 kA at $\tau_{\text{ext}} = 0.3$. The confinement improves with increasing iota. A thermal collapse induced by tearing modes occurs when $\tau = 1/2$ is formed in the gradient region.

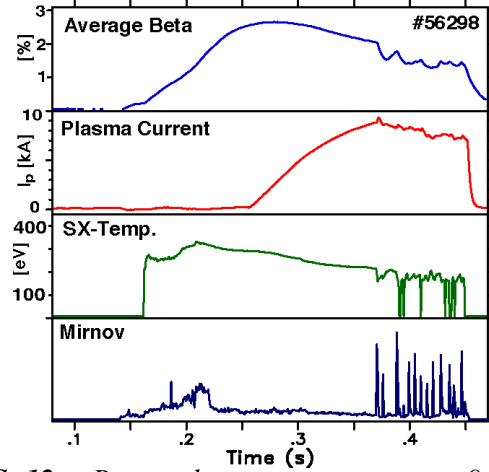


FIG. 12. : Reversed current ramp up to $+9$ kA at $\tau_{\text{ext}} = 0.52$. The confinement deteriorates with decreasing iota. The repetitive fast MHD crashes seem to be connected with a critical temperature.

driven modes. With regard to new stellarator concepts such as the quasi-axisymmetric stellarator [11], where the bootstrap current shall provide a significant contribution to the rotational transform, the role of current driven MHD could be an issue as well. While net-current free operation is maintained in the usual experimental scenario by compensating these currents by a typically small ohmic current (up to about 3 kA under high- β conditions), we have applied OH-current ramps in co- and counter-directions up to 20 kA. Similar current ramp experiments have been conducted earlier in W7-AS under low- β conditions in order to assess the stabilizing effect of the external rotational transform on tearing modes and disruptions [1,12]. In the present experiments the external rotational transform was varied in the range $\tau_{\text{ext}}(a) = 0.26 \dots 0.62$, which is given by the achievement of proper high- β target plasmas and the tolerable magnetic forces between the modular and toroidal field coils. As shown in *FIG. 11*, at first the confinement improves with increasing OH-current generated rotational transform, likely because of the improving high- β equilibrium properties, and β -values of $\langle \beta \rangle \leq 2.9$ % (at $B = 1.25$ T) are reached. But then $\tau = 1/2$ is formed inside the plasma, and when it is pushed towards the gradient region, MHD induced thermal collapses occur in all cases. These MHD events have been studied in more detail by X-ray and magnetic probe measurements. In comparison with the already mentioned studies at low β very similar features concerning the precursor activity, the energy quench phase and the effect on the plasma current have been found. Although these studies are not yet completed our tentative conclusion is, that the collapse of the energy is caused by the onset of growing and rotating $(m,n) = (2,1)$ tearing modes at $\tau = 1/2$, growing to very large perturbations within a few milliseconds. The temporal evolution and the corresponding spatial structure obtained from X-ray tomography is also shown in *FIG. 11*. In spite of the considerable energy and particle loss induced by the mode activity, the plasma equilibrium is maintained due to the external stellarator field, and the plasma current can be raised further.

An example of a reversed current drive case is shown in *FIG. 12*. Here the optimum external rotational transform of $\tau_{\text{ext}} = 0.52$ (see *FIG. 3*) was used for the target plasma. During the current ramp iota is decreased progressively, and therefore the confinement degrades. When the central electron

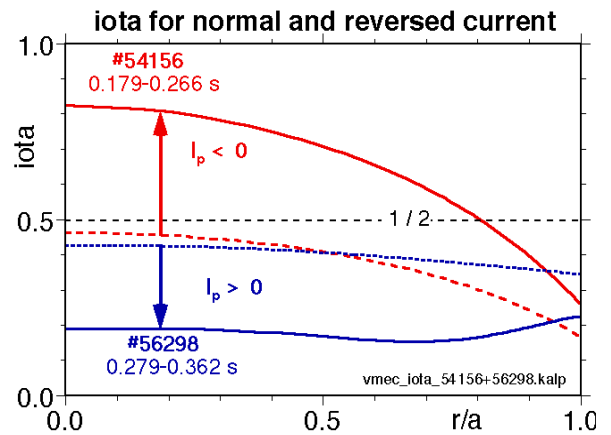


FIG. 13. : Evolution of the profiles of the rotational transform during the current ramps from VMEC for the cases shown in *FIGS. 11, 12*.

temperature has decreased to ≈ 200 eV a series of very fast MHD bursts sets in. The origin of these instabilities, which are also seen without toroidal currents, is not yet understood (see discussion at the end of section 4), but they are definitely not tearing modes. Using counter-currents, configurations with low total rotational transform and flat or marginally reversed iota profiles can be realized as shown in *FIG. 13* (case of *FIG. 11*). These are compared with enhanced shear profiles obtained by co-current drive (case of *FIG. 12*).

6. Summary and Conclusions.

Major changes of W7-AS components have resulted in enhanced performance in the high- β regime with the achievement of volume averaged β -values of up to $\langle\beta\rangle = 3.4\%$ in quasi-stationary discharges at low impurity radiation levels. The replacement of the rotational transform by an equivalent toroidal current would yield a tokamak normalized β -value of $\beta_N \approx 4\dots 9$. This success is attributed to the combination of three technical improvements: firstly, the possibility of injecting all the power in co-direction (co-injection in W7-AS means the direction opposite to the toroidal field, in which case the beam driven current increases the rotational transform); secondly, the possibility of smoothing the flux surfaces at the edge to increase the effective plasma volume and hence to exploit the favourable equilibrium and confinement properties at high-iota; and thirdly, the beneficial effect of limiting the plasma tightly by the graphite covered divertor structure.

The global confinement in the high- β regime shows features of the HDH mode. The confinement times are in the range expected from the W7-scaling. The predicted basic properties of the high- β equilibria are consistent with experimental data obtained from X-ray tomography. The equilibrium β -limit has not yet been reached in the case of high-iota configurations.

A surprising result is that no evidence of a β stability limit is found in general, and only weak MHD-activity is seen in the range of maximum β . The improvement of the stability with increasing β , however, is also reflected in the MHD stability calculations including the evaluation of the Mercier- and resistive interchange criteria, the global ideal mode calculations and the analysis of the local ideal ballooning stability. A key effect seems to be the deepening of the magnetic well and the increase of shear with increasing β . The role of resistive modes is not yet clear and will be investigated further. As far as the effect of toroidal currents on the high- β performance is concerned, additional operational limits for stellarator-tokamak hybrid devices due to tearing modes can exist. They may be overcome by avoiding low order rational surfaces at the edge. The results concerning the achievable plasma β in W7-AS are believed to be of great significance for the stellarator approach to a fusion reactor. In particular, the studies result in increased confidence in the projection of the equilibrium and stability properties in the W7-X stellarator, which is presently under construction.

References

- [1] A. Weller et al., Phys. Plasmas **8**, 931 (2001).
- [2] F. Wagner et al., paper **OV/2-4**, this conference.
- [3] P. Grigull et al., Plasma Phys. Control. Fusion **43**, A175 (2001).
- [4] K. McCormick et al., Phys. Rev. Lett. **89**, 015001 (2002).
- [5] L. Giannone et al., Plasma Phys. Control. Fusion **42**, 603 (2000).
- [6] U. Stroth et al., Nuclear Fusion **36**, 1063 (1996).
- [7] S.P. Hirshman et al., Comput. Phys. Commun. **43**, 143 (1986).
- [8] J. Nührenberg and R. Zille, in Theory of Fusion Plasmas, Varenna 1987, 3 (1988).
- [9] C. Schwab, Phys. Fluids B **5**, 3195 (1993).
- [10] R. Sanchez et al., J. Comput. Phys. **161**, 576 (2000).
- [11] M. Zarnstorff et al., Plasma Phys. Control. Fusion **43**, A237 (2001).
- [12] Sallander, E. and Weller, A., Nuclear Fusion **40**, 1499 (2000).